Structural change of ionic association in ionic liquid/water mixtures: A high-pressure infrared spectroscopic study

Yasuhiro Umebayashi, Jyh-Chiang Jiang, Yu-Lun Shan, Kuan-Hung Lin, Kenta Fujii, Shiro Seki, Shin-Ichi Ishiguro, Sheng Hsien Lin, and Hai-Chou Chang

Citation: The Journal of Chemical Physics **130**, 124503 (2009); doi: 10.1063/1.3100099
View online: http://dx.doi.org/10.1063/1.3100099
View Table of Contents: http://scitation.aip.org/content/aip/journal/jcp/130/12?ver=pdfcov
Published by the AIP Publishing

Structural change of ionic association in ionic liquid/water mixtures: A high-pressure infrared spectroscopic study

Yasuhiro Umebayashi,[1] Jyh-Chiang Jiang,[2] Yu-Lun Shan,[3] Kuan-Hung Lin,[3] Kenta Fujii,[4] Shiro Seki,[5] Shin-Ichi Ishiguro,[1] Sheng Hsien Lin,[6,7] and Hai-Chou Chang[3,a)]
[1]*Department of Chemistry, Faculty of Science, Kyushu University, Hakozaki, Higashi-ku, Fukuoko 812-8581, Japan*
[2]*Department of Chemical Engineering, National Taiwan University of Science and Technology, Taipei 106, Taiwan*
[3]*Department of Chemistry, National Dong Hwa University, Shoufeng, Hualien 974, Taiwan*
[4]*Department of Chemistry and Applied Chemistry, Faculty of Science and Engineering, Saga University, Honjo-machi, Saga 840-8502, Japan*
[5]*Material Science Research Laboratory, Central Research Institute of Electric Power Industry, Komae, Tokyo 201-8511, Japan*
[6]*Department of Applied Chemistry, National Chiao Tung University, Hsinchu 30010, Taiwan*
[7]*Institute of Atomic and Molecular Sciences, Academia Sinica, P.O. Box 23-166, Taipei 106, Taiwan*

(Received 4 December 2008; accepted 25 February 2009; published online 24 March 2009)

High-pressure infrared measurements were carried out to observe the microscopic structures of two imidazolium-based ionic liquids, i.e., 1-ethyl-3-methylimidazolium bis(trifluoromethylsulfonyl)amide $[EMI^+(CF_3SO_2)_2N^-$, $EMI^+TFSA^-]$ and 1-ethyl-3-methylimidazolium bis(fluorosulfonyl)amide $[EMI^+(FSO_2)_2N^-$, $EMI^+FSA^-]$. The results obtained at ambient pressure indicate that the imidazolium C–H may exist in two different forms, i.e., isolated and network structures. As the sample of pure EMI^+FSA^- was compressed, the network configuration is favored with increasing pressure by debiting the isolated form. For EMI^+TFSA^-/H_2O mixtures, the imidazolium C–H peaks split into four bands at high pressures. The new spectral features at approximately 3117 and 3190 cm^{-1}, being concentration sensitive, can be attributed to the interactions between the imidazolium C–H and water molecules. The alkyl C–H absorption exhibits a new band at approximately 3025 cm^{-1} under high pressures. This observation suggests the formation of a certain water structure around the alkyl C–H groups. The O–H stretching absorption reveals two types of O–H species, i.e., free O–H and bonded O–H. For EMI^+TFSA^-/H_2O mixtures, the compression leads to a loss of the free O–H band intensities, and pressure somehow stabilizes the bonded O–H configurations. The results also suggest the non-negligible roles of weak hydrogen bonds in the structure of ionic liquids. © *2009 American Institute of Physics*. [DOI: 10.1063/1.3100099]

I. INTRODUCTION

In recent years, room-temperature ionic liquids have attracted considerable interest as green recyclable alternatives to the traditional organic solvents.[1–5] Interest in investigating the properties and applications of ionic liquids has been intensified owing to their dual nature as both salts and fluids. The most extensively studied ionic liquids are the 1-alkyl-3-methylimidazolium salts.[1–3] Due to the large size and conformational flexibility of the cations, the liquid state is thermodynamically favorable. This leads to small lattice enthalpies and large entropy changes that result in a melting temperature around room temperature. The unique properties of ionic liquids allow their use in several applications in chemical industry such as solvents in organic synthesis as homogeneous and biphasic transfer catalysts and in electrochemistry.[1,2] Ionic liquids have been employed as mixtures with other classic solvents, and this use calls for an understanding of the ionic liquid-classic solvent interactions.[6–14] Ionic liquids based on hydrophobic ions such as imidazolium derivatives and anions such as bis(trifluoromethylsulfonyl)amide $(TFSA^-, [(CF_3SO_2)_2N^-])$ form biphasic systems with water and can be used in separation processes.[1,2] The bis(trifluoromethylsulfonyl)amide anion is also called NTf_2^-, Tf_2N^-, and $TFSI^-$ in the literature. For the extraction of organic products from aqueous media, ionic liquids with low water solubility are required. Therefore, the knowledge of the interactions of water and ionic liquids prior to their industrial applications is of primary importance. Increasing attention has been devoted to conducting biocatalytic transformation in ionic liquids.[15] The addition of water to ionic liquids is very common in biocatalytic work, and this is one of motivations for the current work.[15,16]

Spectroscopic methods have been widely applied to ionic liquids to probe their dynamics, structures, interactions, solvation, and transport. Measurements of the solvation responses and microscopic solvent properties have resulted in the accumulation of a sizable database on solvation dynamics in ionic liquids.[17–21] For example, several groups have

a)Author to whom correspondence should be addressed. Electronic mail: hcchang@mail.ndhu.edu.tw. FAX: +886-3-8633570. Tel.: +886-3-8633585.

used the femtosecond optical heterodyne-detected Raman-induced Kerr effect spectroscopy (OHD-RIKES) method to characterize the dynamics in ionic liquids.[5] Since the early pioneering work based on the fluorescence behavior of C153 in ionic liquids,[22] several researchers have studied salvation dynamics in ionic liquids.[18,20,23] Most of these studies have indicated that the time-resolvable part of the dynamics is biphasic or nonexponential in nature. Solvation dynamics in mixed solvents containing ionic liquids has also been probed.[24–27] Previous studies to the structure of ionic liquids have included the use of x-ray crystallography. Although the results of crystal structures are highly informative on the relative geometry changes, crystallography does not provide direct information on the local structure in the liquid state. Thus, experimental techniques, such as IR and Raman spectroscopy, were often used to explore hydrogen-bonding structures of liquid mixtures. Over the past years the interest in pressure as an experimental variable has been growing in physicochemical studies.[8,28–30] The study of pressure effects reveals the intermolecular interactions of the ionic liquid at a constant kinetic energy or temperature.

The role of water in ionic liquids is complex and depends on the supramolecular structures of ionic liquids. By studying water-induced acceleration of ion diffusion, Schroder *et al.*[31] proposed that imidazolium-based ionic liquids have polar and nonpolar regions. Alkyl imidazolium cations with long enough alkyl chain length ($n \geq 4$) were characterized by the existence of structural organization at the nanometer scale, as reported by Triolo *et al.*[32] At high ionic liquid concentrations, ionic liquids seem to form clusters, as in the pure state, and water molecules interact with the clusters without interacting among themselves. Therefore, ionic liquids containing dissolved water may not be regarded as homogeneous solvents but have to be considered as nanostructured materials.[33] Interactions of water dissolved in ionic liquids have been extensively studied using infrared spectroscopy. In particular, the O–H stretching modes of water are sensitive to the environment and intermolecular interactions. Based on attenuated total reflectance infrared measurements, researchers concluded that anions are responsible for the interactions of ionic liquids and water.[34] Despite the numerous computational and experimental studies on ionic liquid/water mixtures, our knowledge of the interaction between water and ionic liquids remains somewhat empirical.

Various studies have been made to elucidate the role of weak hydrogen bonds, such as C–H···O and C–H···X, in the structure of ionic liquids.[35,36] The observation of the C–H stretching vibration is one of the keys to characterize the presence of such a weak hydrogen bond and can serve as a useful probe to reflect the interactions between ionic liquids and water. One of the intriguing aspects of weak hydrogen bonds is that the C–H stretching band undergoes a blueshift when the C–H groups form weak hydrogen bonds.[37–39] This behavior is opposite to that of the classical hydrogen bond, and its underlying mechanism is still under debate.[37–39] One of the reasons for this controversy is the weakness of weak hydrogen bonds. Conclusive experimental evidence for the main origin of the blueshifts is difficult to obtain because weak hydrogen bonds usually coexist with other strong interactions and are typically weak. Therefore, methods that enhance weak hydrogen bonding are crucial to provide scientists with a clear and unified view of this important phenomenon. Studies have shown the potential significance that pressure has on controlling the strength of weak hydrogen bonds.[28–30] In this study, we show that high pressure is a sensitive method to probe weak hydrogen bonds in ionic liquid mixtures.

The effects of high pressure on intermolecular interactions have been the subject of extensive studies. Application of high pressure is the ideal tool to tune continuously the bonding properties of the materials. Pressure affects chemical equilibrium, and the reaction volume is defined by the standard equation, $\Delta V = -[RT\partial \ln K/\partial P]_T$.[40] If a system is compressed, then the reaction will adjust to favor the components with smaller volume ($\Delta V < 0$). The pressure-induced changes in the vibrational characteristics are of particular interest. They yield important information on the bonding properties, especially with regard to the interplay of covalent and hydrogen bonding.

II. EXPERIMENTAL SECTION

Samples were prepared using 1-ethyl-3-methylimidazolium bis(trifluoromethylsulfonyl)amide (98.85% by HNMR, LOT1257559, Fluka), D_2O (99.9%, Aldrich), H_2O (for chromatography, Merck), and methanol-d_4 (99.8% D, Cambridge Isotope). 1-ethyl-3-methylimidazolium bis(fluorosulfonyl)amide of spectroscopic grade (Dai-ichi Kogyo Seiyaku Co. Ltd.) was used without further purification.[41] A diamond anvil cell (DAC) of Merril–Bassett design, having a diamond culet size of 0.6 mm, was used for generating pressures up to approximately 2 GPa. Two type-IIa diamonds were used for midinfrared measurements. The sample was contained in a 0.3-mm-diameter hole in a 0.25-mm-thick Inconel gasket mounted on the DAC. To reduce the absorbance of the samples, CaF_2 crystals (prepared from a CaF_2 optical window) were placed into the holes and compressed firmly prior to inserting the samples. A droplet of a sample filled the empty space of the entire hole of the gasket in the DAC, which was subsequently sealed when the opposed anvils were pushed toward one another. Infrared spectra of the samples were measured on a PerkinElmer Fourier transform spectrophotometer (model Spectrum RXI) equipped with a lithium tantalite midinfrared detector. The infrared beam was condensed through a 5X beam condenser onto the sample in the DAC. Typically, we chose a resolution of 4 cm^{-1} (data point resolution of 2 cm^{-1}). For each spectrum, typically 1000 scans were compiled. To remove the absorption of the diamond anvils, the absorption spectra of DAC were measured first and subtracted from those of the samples. Pressure calibration follows Wong's method.[42,43] The pressure dependence of screw moving distances was measured.

III. RESULTS AND DISCUSSION

Figure 1 displays infrared spectra of pure 1-ethyl-3-methylimidazolium bis(trifluoromethylsulfonyl)amide (EMI^+TFSA^-) obtained under ambient pressure (curve

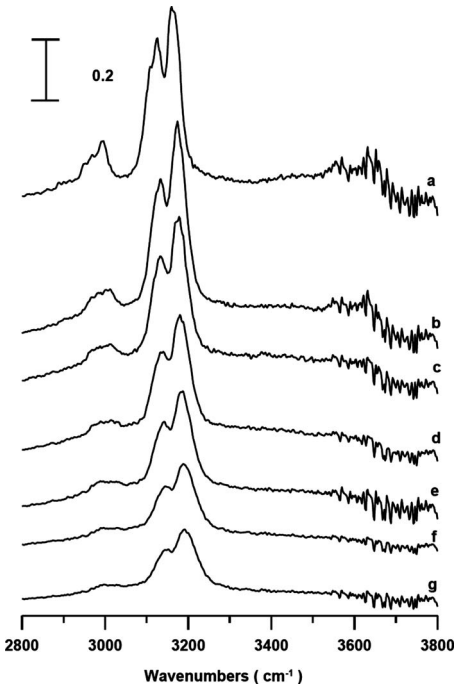

FIG. 1. IR spectra of pure EMI^+TFSA^- under (a) ambient pressure and at (b) 0.3, (c) 0.9, (d) 1.5, (e) 1.9, (f) 2.3, and (g) 2.5 GPa.

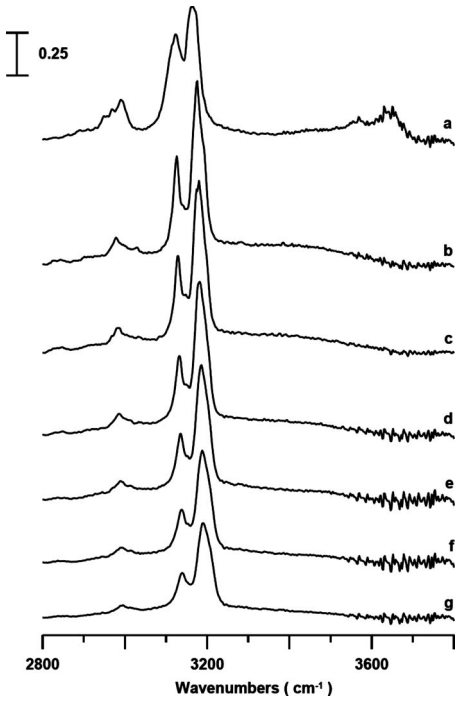

FIG. 2. Pressure dependence of IR spectra of pure EMI^+FSA^- under (a) ambient pressure and at (b) 0.3, (c) 0.9, (d) 1.5, (e) 1.9, (f) 2.3, and (g) 2.5 GPa.

a) and at 0.3 (curve b), 0.9 (curve c), 1.5 (curve d), 1.9 (curve e), 2.3 (curve f), and 2.5 GPa (curve g). As indicated in Fig. 1(a), the aliphatic C–H modes of the methyl and ethyl groups are seen at 2951, 2970, and 2992 cm^{-1}. The peaks at approximately 3124 and 3162 cm^{-1} are assigned to coupled C–H stretching modes of C^2–H, C^4–H, and C^5–H on the imidazolium cation. The imidazolium C–H stretching absorption has two major peaks; close examinations reveal more structures. The nearly degenerated peaks may be attributed to the perturbation of neighboring ions in the liquid state. This observation is consistent with the suggestions that the imidazolium C–H may exist in two different forms, i.e., isolated and network structures.[44,45] As the sample was compressed, that is, increasing the pressure from ambient [Fig. 1(a)] to 0.3 GPa [Fig. 1(b)], the imidazolium C–H bands were blueshifted to 3133 and 3174 cm^{-1}, respectively. As the sample was further compressed [Figs. 1(b)–1(g)], we also observed a monotonic blueshift in frequency for the characteristic imidazolium C–H bands. Nevertheless, the pressure-induced frequency shifts of the imidazolium C–H bands are relatively small under pressures above 0.3 GPa. This may indicate a phase transition, i.e., pressure-induced solidification, above a pressure of 0.3 GPa. The blueshift may originate from the overlap repulsion effect enhanced by hydrostatic pressure. The pressure-enhanced C–H···N and C–H···F interactions may be a compensatory mechanism to provide additional stability.

Figure 2 displays infrared spectra of pure 1-ethyl-3-methylimidazolium bis(fluorosulfonyl)amide (EMI^+FSA^-) obtained under ambient pressure (curve a) and at 0.3 (curve b), 0.9 (curve c), 1.5 (curve d), 1.9 (curve e), 2.3 (curve f), and 2.5 GPa (curve g). Figure 2(a) exhibits three bands at 2954, 2971, and 2990 cm^{-1} corresponding to alkyl C–H stretching modes, and the 3124 and 3164 cm^{-1} bands can be attributed to imidazolium C–H stretching vibrations. The C–H stretching modes underwent dramatic changes in their spectral profiles as the pressure was elevated to 0.3 GPa in curve b. As revealed, Fig. 2(b) shows the major alkyl C–H band located at 2980 cm^{-1}, whereas the imidazolium C–H bands are shifted to 3126 and 3177 cm^{-1}. The widths of imidazolium C–H stretching bands decrease in curve b, and this observation is likely related to local structures of the imidazolium ring. The decrease in width may be caused by the loss in intensity of those nearly degenerated bands attributed to the isolated structures. In other words, the network configuration is favored with increasing pressure by debiting the isolated form in Fig. 2(b). Although the present experimental results may be explained by the network-isolated structural equilibrium, we cannot tell much about the speciation. Network species may be ion pairs (or larger ion clusters), and the isolated species may mean the dissociation into free ions (or smaller ion clusters). As the pressure was further elevated, the alkyl and imidazolium C–H bands were blueshifted in Figs. 2(b)–2(g). The monotonic blueshift in frequency for the characteristic C–H bands ($P > 0.3$ GPa) suggests that the network configurations seem to be thermodynamically stable up to the pressure of 2.5 GPa.

In order to gain further insights on the local structures of imidazolium cations, we have studied concentration-dependent variation in the infrared spectra of EMI^+TFSA^-. Figure 3 displays infrared spectra of an EMI^+TFSA^-/H_2O mixture (mole fraction of EMI^+TFSA^-: approximately 0.84) obtained under ambient pressure (curve a) and at 0.3 (curve b), 0.9 (curve c), 1.9 (curve d), and 2.5 GPa (curve e). As revealed in Fig. 3(a), the C–H bands are located at 2953, 2972, 2994, 3123, and 3163 cm^{-1}, and the stretching modes of O–H appear at approximately 3565 and 3630 cm^{-1}. We

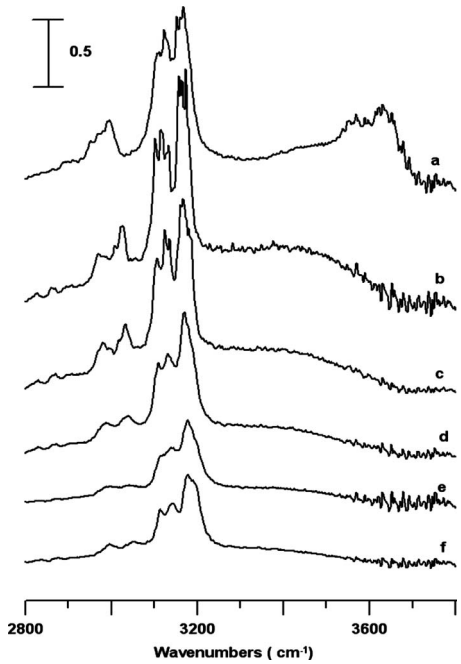

FIG. 3. IR spectra of an EMI^+TFSA^-/H_2O mixture (mole fraction of EMI^+TFSA^-: 0.84) obtained under ambient pressure (curve a) and at 0.3 (curve b), 0.9 (curve c), 1.9 (curve d), and 2.5 GPa (curve e). Curve f shows the IR spectra of a solution of mole fraction $(EMI^+TFSA^-)=0.7$ obtained at 2.5 GPa.

observe no drastic changes in the concentration dependence of the alkyl and imidazolium C–H band frequency at high concentrations of EMI^+TFSA^-; that is, mole fraction $(EMI^+TFSA^-)\geq 0.84$ [cf. Figs. 1(a) and 3(a)]. This behavior may indicate a slight perturbation of local structures due to the presence of H_2O at ambient pressure. According to Cammarata *et al.*[34] and Lopez-Pastor *et al.*,[46] the two well-separated bands observed at 3565 and 3630 cm^{-1} can be assigned to the antisymmetric (ν_3) and symmetric (ν_1) stretch vibrations of the water monomer or free O–H interacting with anions. As the mixture was compressed, i.e., increasing the pressure from ambient [Fig. 3(a)] to 0.9 GPa [Fig. 3(b)], a loss of the free O–H band intensities was observed. The bonded O–H band appears as a broad feature at approximately 3400 cm^{-1} in Figs. 3(b)–3(g). It appears that pressure somehow stabilizes the bonded O–H conformation, as free O–H is likely switched to bonded O–H as high pressures are applied in Fig. 3. Evolution of the O–H spectral features in Fig. 3 may arise from changes in the local structures of water molecules, and the geometric properties of the hydrogen-bond network are likely perturbed as the pressure is elevated. We stress that the alkyl C–H stretching absorption exhibits a new band at 3025 cm^{-1} associated with a weak shoulder at 3009 cm^{-1} in Fig. 3(b). We notice that no more vibration modes exist in this region, so this spectral feature located at approximately 3025 cm^{-1}, being sensitive to concentration and pressure dependence, may be assumed to arise from the interaction between alkyl C–H and H_2O, i.e., C–H···O interaction. It is well known that the C–H covalent bond tends to shorten as a result of the formation of a hydrogen bond with a Lewis base.[37–39] This observation suggests the formation of a certain water structure around the alkyl C–H groups, but the details remain unclear.

The ring C–H stretching absorption shows four peaks under high pressure in Fig. 3. For example, the imidazolium C–H peaks split into four bands located at 3117, 3141, 3179, and 3190 cm^{-1} (a weak shoulder) in Fig. 3(e). In order to learn the insight of the new spectral features revealed in the imidazolium C–H region, further pressure study on various amounts of EMI^+TFSA^-/H_2O provides direct evidence. Figure 3(f) shows the IR spectra of a solution of mole fraction $(EMI^+TFSA^-)=0.7$ obtained under the pressure of 2.5 GPa. See also Fig. S1 in Supplemental Material for more pressure-dependent results.[47] As revealed in Fig. 3(f), the increases in intensities were observed for the bands at 3117 and 3190 cm^{-1}. Comparing these spectra features in Fig. 3(e) with those in Fig. 3(f), the 3117 and 3190 cm^{-1} components, being concentration sensitive, can be attributed to the interactions between the imidazolium C–H and water molecules. The lower (redshift) frequency for the 3117 cm^{-1} component can be physically related to the well-known acidity of imidazolium C^2–H. In the past, several models have been proposed for the theoretical understanding of the C–H···O interactions. When a molecule that is capable of forming blueshifting hydrogen bonding binds to a site with a sufficiently strong electrostatic field to dominate over the overlap effect, that molecule is predicted to display a redshifting hydrogen bond. In this article, we present a means of looking at this issue by employing the high-pressure method. It is instructive to point out that the shifts in C–H stretches may due to the replacement of an interaction between the C–H and an anion with an interaction with water. In other words, the redshift in C^2–H appears to be the difference between two redshifts.

Figure 4 displays infrared spectra of an EMI^+TFSA^-/methanol-d_4 mixture having a mole fraction of EMI^+TFSA^- equal to 0.2 obtained under ambient pressure (curve a) and at 0.3 (curve b), 0.9 (curve c), 1.5 (curve d), 1.9 (curve e), 2.3 (curve f), and 2.5 GPa (curve g). In order to reduce the O–H absorption intensity, we measured the infrared spectrum in a solution of methanol-d_4 (with minimal methanol as the impurity), rather than methanol (Fig. 4). The bonded O–H band appears as a broad feature at approximately 3400 cm^{-1}, and the shoulder at approximately 3560 cm^{-1} is assigned to free O–H stretching vibration in Fig. 4(a). This result indicates that at least two different types of O–H species were observed in Fig. 4(a), and the prominent O–H species is the bonded O–H. As the sample was compressed [Figs. 4(b)–4(g)], we observe blueshifts in frequency for the imidazolium C–H and redshifts in frequency for the bonded O–H in Fig. 4. Nevertheless, the free O–H stretching band does not change its position with pressure. The presence of the shoulder at approximately 3560 cm^{-1} in Figs. 4(b)–4(g) indicates that the free O–H is still stable under high pressure. This observation is remarkably different from the results of EMI^+TFSA^-/H_2O (Fig. 3). Water molecules tend to form three-dimensional hydrogen-bonding structures, but molecules in pure methanol associate with each other to form short chains with an average chain length of five or so molecules.[48] It is also known that hydrogen-

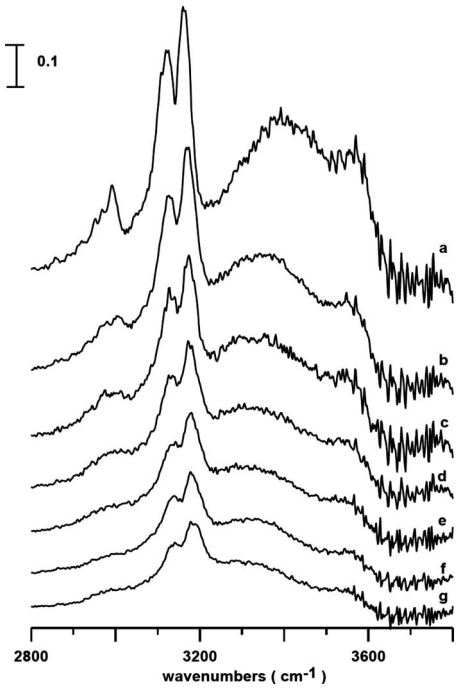

FIG. 4. IR spectra of an EMI^+TFSA^-/methanol-d_4 mixture having mole fraction of EMI^+TFSA^- equal to 0.2 obtained under ambient pressure (curve a) and at 0.3 (curve b), 0.9 (curve c), 1.5 (curve d), 1.9 (curve e), 2.3 (curve f), and 2.5 GPa (curve g).

bond cooperativity due to concerted charge transfer can greatly enhance the strength of the individual hydrogen bonds involved in the coupling.[28–30] Attention has been paid to the cooperative effect with increasing cluster size.[36] Thus, the cluster size may be one of the reasons for the unique behavior of added methanol-d_4 observed in Fig. 4.

Figure 5 displays the optimized density functional theory–calculated structures of EMI^+FSA^- ion pairs [Figs. 5(a)–5(d)] and ion-pair dimers [Figs. 5(e) and 5(f)]. It was known that the $TFSA^-$ anion shows similar intensities of both the *trans* and *cis* conformers as revealed in OHD-RIKES spectra.[5] For the purpose of comparison with previous $TFSA^-$ calculation,[44] we only show the calculation results of the *trans* conformer in Fig. 5. All calculations were performed by using the GAUSSIAN 03 program package.[49] We employed the B3LYP functional together with a standard 6-31+G* basis set. All geometries were determined on the counterpoise (CP)-optimized surfaces. Energy results are shown in Table I. As illustrated in Figs. 5(a)–5(d), the C^2–H and $C^{4,5}$–H can be involved in hydrogen bonding in ion pairs. Based on energy results revealed in Table I, the energetically favored approach for the anion to interact with the imidazolium cation is through the formation of C^2–H···O [Fig. 5(c)] or C^2–H···N^- [Fig. 5(d)]. This finding is in agreement with the observation that the C^2–H group has a larger positive charge than the C^4–H and C^5–H groups. It is known that cohesion in ionic liquids is strong and mostly electrostatic. Nevertheless, this study elucidates the non-negligible role of weak hydrogen bonds, such as C–H···O and C–H···N, in the structures of ionic liquids. As the clusters increase in size, the structural identification of the isomers is complicated by numerous different isomeric configurations. Only two of the optimized structures of ion-pair dimers are reported in Figs. 5(e) and 5(f). As shown in Table I, interaction energies of ion-pair dimers [Figs. 5(e) and 5(f)] are approximately 2.1 times of those of ion pairs [Figs. 5(c) and 5(d)]. In other words, ion-pair dimers are only slightly favored over ion pairs for interaction-energy reasons. However, ion pairs might be entropically favored over ion-pair dimers. Koddermann *et al.*[44] calculated local minima structures for ion pairs and ion-pair dimers of EMI^+TFSA^-. The predicted interaction energies of EMI^+TFSA^- (Koddermann

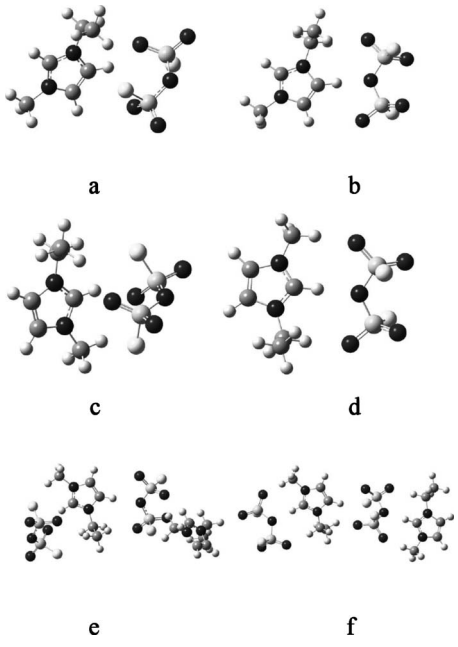

FIG. 5. Optimized structures of [(a)–(d)] the EMI^+FSA^- monomer and [(e) and (f)] the EMI^+FSA^- dimer.

TABLE I. Calculated relative energies (hartree/mol), basis set superposition error (BSSE) (hartree/mol), and total interaction energies (kcal/mol).

Species[a–c]	Relative energies	BSSE	$-\Delta E$
FSA^-	−1351.680 449		
$EMIM^+$	−344.385 267		
a	−1696.171 386	0.002 058	65.0
b	−1696.171 279	0.002 512	64.7
c	−1696.183 195	0.002 596	72.1
d	−1696.182 919	0.002 801	71.8
e	−3392.381 702	0.006 486	153.0
f	−3392.382 371	0.006 773	153.2

[a]Structures illustrated in Fig. 5.
[b]FSA^-: $[(FSO_2)_2N^-]$.
[c]$EMIM^+$:

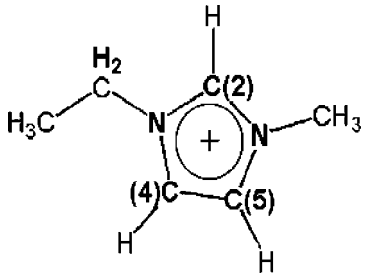

et al., Table I)[44] and EMI^+FSA^- complexes (this study, Table I) are very similar. We also calculated the natural bond orbital (NBO) charges of $TFSA^-$ and FSA^- monomers. The average NBO charges of F atoms in $TFSA^-$ and FSA^- are equal to -0.36 and -0.51, respectively. These results may indicate the non-negligible role of the C–H···F interactions in EMI^+FSA^-. The stronger C–H···F interactions in EMI^+FSA^- may be one of the reasons for the remarkable differences in the pressure-dependent results of EMI^+TFSA^- (Fig. 1) and EMI^+FSA^- (Fig. 2).

IV. CONCLUSION

We have used the concentration and pressure-dependent IR techniques to monitor the structures of EMI^+TFSA^- and EMI^+FSA^-. Our results indicate that the imidazolium C–H may exist in two different forms, i.e., isolated and network structures at ambient pressure. Network species may be ion pairs (or larger ion clusters), and the isolated species may mean the dissociation into free ions (or smaller ion clusters). As neat EMI^+FSA^- was compressed, the network configuration is favored with increasing pressure. As EMI^+TFSA^-/H_2O mixtures were compressed, the alkyl C–H absorption exhibits a new band at approximately 3025 cm^{-1} and the imidazolium C–H revealed new spectra features at approximately 3117 and 3190 cm^{-1}. These new peaks can be attributed to the interactions between the C–H and water molecules. This observation suggests the formation of a certain water structure around the alkyl and imidazolium C–H groups under high pressures. For EMI^+TFSA^-/H_2O mixtures, free O–H is switched to bonded O–H as high pressures are applied. However, the free O–H is still stable under high pressures for the methanol mixtures.

ACKNOWLEDGMENTS

The authors thank the National Dong Hwa University and the National Science Council of Taiwan (Contract No. NSC 95-2113-M-259-013-MY3) for financial support. This work has been financially supported by Grant-in-Aids for Scientific Research Nos. 18850017, 19003963, 19350033, and 20350037 from the Ministry of Education, Culture, Sports, Science and Technology, Japan.

[1] *Green Industrial Applications of Ionic Liquids*, NATO Science Series, edited by R. D. Rogers, K. R. Seddon, and S. Volkov (Kluwer, Dordrecht, 2002).
[2] *Ionic Liquids in Synthesis*, edited by P. Wasserscheid and T. Welton (Wiley VCH, Weinheim, 2002).
[3] H. Weingartner, Angew. Chem., Int. Ed. **47**, 654 (2008).
[4] C. Hardacre, J. D. Holbrey, M. Nieuwenhuyzen, and T. G. A. Youngs, Acc. Chem. Res. **40**, 1146 (2007).
[5] E. W. Castner, Jr., J. F. Wishart, and H. Shirota, Acc. Chem. Res. **40**, 1217 (2007).
[6] C. Schroder, T. Rudas, G. Neumayr, S. Benkner, and O. Steinhauser, J. Chem. Phys. **127**, 234503 (2007).
[7] D. Paschek, T. Koddermann, and R. Ludwig, Phys. Rev. Lett. **100**, 115901 (2008).
[8] H. C. Chang, J. C. Jiang, Y. C. Liou, C. H. Hung, T. Y. Lai, and S. H. Lin, J. Chem. Phys. **129**, 044506 (2008).
[9] M. Blesic, A. Lopes, E. Melo, Z. Petrovski, N. V. Plechkova, J. N. C. Lopes, K. R. Seddon, and L. P. N. Rebelo, J. Phys. Chem. B **112**, 8645 (2008).
[10] M. G. Freire, P. J. Carvalho, R. L. Gardas, I. M. Marrucho, L. M. N. B. F. Santos, and J. A. P. Coutinho, J. Phys. Chem. B **112**, 1604 (2008).
[11] K. S. Mali, G. B. Dutt, and T. Mukherjee, J. Chem. Phys. **128**, 054504 (2008).
[12] K. Behera, M. D. Pandey, M. Porel, and S. Pandey, J. Chem. Phys. **127**, 184501 (2007).
[13] Y. Jeon, J. Sung, D. Kim, C. Seo, H. Cheong, Y. Ouchi, R. Ozawa, and H. Hamaguchi, J. Phys. Chem. B **112**, 923 (2008).
[14] T. Koddermann, C. Wertz, A. Heintz, and R. Ludwig, Angew. Chem., Int. Ed. **45**, 3697 (2006).
[15] R. A. Sheldon, Green Chem. **7**, 267 (2005).
[16] R. A. Sheldon, R. M. Lau, M. J. Sorgedrager, F. van Rantwijk, and K. R. Seddon, Green Chem. **4**, 147 (2002).
[17] J. H. Werner, S. N. Baker, and G. A. Baker, Analyst (Cambridge, U.K.) **128**, 786 (2003).
[18] S. Arzhantsev, H. Jin, G. A. Baker, and M. Maroncelli, J. Phys. Chem. B **111**, 4978 (2007).
[19] S. N. Baker, G. A. Baker, and F. V. Bright, Green Chem. **4**, 165 (2002).
[20] D. Seth, S. Sarkar, and N. Sarkar, J. Phys. Chem. B **112**, 2629 (2008).
[21] A. Sarkar and S. Pandey, J. Chem. Eng. Data **51**, 2051 (2006).
[22] R. Karmakar and A. Samanta, J. Phys. Chem. A **106**, 4447 (2002).
[23] P. Mukherjee, J. A. Crank, P. S. Sharma, A. B. Wijeratne, R. Adhikary, S. Bose, D. W. Armstrong, and J. W. Petrich, J. Phys. Chem. B **112**, 3390 (2008).
[24] A. Paul and A. Samanta, J. Phys. Chem. B **112**, 947 (2008).
[25] W. E. Gardinier, G. A. Baker, S. N. Baker, and F. V. Bright, Macromolecules **38**, 8574 (2005).
[26] D. Chakrabarty, A. Chakraborty, D. Seth, P. Hazra, and N. Sarkar, Chem. Phys. Lett. **397**, 469 (2004).
[27] H. V. R. Annapureddy, Z. Hu, J. Xia, and C. J. Margulis, J. Phys. Chem. B **112**, 1770 (2008).
[28] H. C. Chang, J. C. Jiang, C. Y. Chang, J. C. Su, C. H. Hung, Y. C. Liou, and S. H. Lin, J. Phys. Chem. B **112**, 4351 (2008).
[29] H. C. Chang, J. C. Jiang, J. C. Su, C. Y. Chang, and S. H. Lin, J. Phys. Chem. A **111**, 9201 (2007).
[30] H. C. Chang, J. C. Jiang, W. C. Tsai, G. C. Chen, and S. H. Lin, J. Phys. Chem. B **110**, 3302 (2006).
[31] U. Schroder, J. D. Wadhawan, R. G. Compton, F. Marken, P. A. Z. Suarez, C. S. Consorti, R. F. de Souza, and J. Dupont, New J. Chem. **24**, 1009 (2000).
[32] A. Triolo, O. Russina, H. J. Bleif, and E. Di Cola, J. Phys. Chem. B **111**, 4641 (2007).
[33] W. Jiang, Y. Wang, and G. A. Voth, J. Phys. Chem. B **111**, 4812 (2007).
[34] L. Cammarata, S. G. Kazarian, P. A. Salter, and T. Welton, Phys. Chem. Chem. Phys. **3**, 5192 (2001).
[35] A. Mele, C. D. Tran, and S. H. De Paoli Lacerda, Angew. Chem., Int. Ed. **42**, 4364 (2003).
[36] S. Koβmann, J. Thar, B. Kirchner, P. A. Hunt, and T. Welton, J. Chem. Phys. **124**, 174506 (2006).
[37] P. Hobza and Z. Havlas, Chem. Rev. (Washington, D.C.) **100**, 4253 (2000).
[38] Y. L. Gu, T. Kar, and S. Scheiner, J. Am. Chem. Soc. **121**, 9411 (1999).
[39] A. Masunov, J. J. Dannenberg, and R. H. Contreras, J. Phys. Chem. A **105**, 4737 (2001).
[40] J. Jonas and A. Jonas, Annu. Rev. Biophys. Biomol. Struct. **23**, 287 (1994).
[41] K. Fujii, S. Seki, S. Fukuda, R. Kanzaki, T. Takamuku, Y. Umebayashi, and S. Ishiguro, J. Phys. Chem. B **111**, 12829 (2007).
[42] P. T. T. Wong, D. J. Moffatt, and F. L. Baudais, Appl. Spectrosc. **39**, 733 (1985).
[43] P. T. T. Wong and D. J. Moffatt, Appl. Spectrosc. **41**, 1070 (1987).
[44] T. Koddermann, C. Wertz, A. Heintz, and R. Ludwig, ChemPhysChem **7**, 1944 (2006).
[45] A. Yokozeki, D. J. Kasprzak, and M. B. Shiflett, Phys. Chem. Chem. Phys. **9**, 5018 (2007).
[46] M. Lopez-Pastor, M. J. Ayora-Canada, M. Valcarcel, and B. Lendl, J. Phys. Chem. B **110**, 10896 (2006).
[47] See EPAPS Document No. E-JCPSA6-130-008913 for Fig. S1. For more information on EPAPS, see http://www.aip.org/pubservs/epaps.html.
[48] S. Dixit, W. C. K. Poon, and J. Crain, J. Phys.: Condens. Matter **12**, L323 (2000).
[49] M. J. Frish, G. W. Trucks, H. B. Schlegel *et al.*, GAUSSIAN 03, Revision A.7, Gaussian, Inc., Pittsburgh, PA, 2003.